

# Particle Production in Central A+A Collisions at 40, 80, and 158 AGeV

C. Alt<sup>1</sup>, C. Blume<sup>1,2</sup>, R. Bramm<sup>1</sup>, P. Bunčić<sup>1</sup>, P. Dinkelaker<sup>1</sup>, D. Flierl<sup>1</sup>, V. Friese<sup>2</sup>, M. Gaździcki<sup>1</sup>, S. Kniege<sup>1</sup>, T. Kollegger<sup>1</sup>, I. Kraus<sup>2</sup>, C. Meurer<sup>2</sup>, A. Mischke<sup>2</sup>, M. Mitrovski<sup>1</sup>, S. Radomski<sup>2</sup>, R. Renford<sup>1</sup>, A. Sandoval<sup>2</sup>, H. Sann<sup>2</sup>, R. Stock<sup>1</sup>, H. Ströbele<sup>1</sup>, A. Wetzler<sup>1</sup>, I.K. Yoo<sup>2</sup>, and J. Zaraneck<sup>1</sup>

<sup>1</sup>Universität Frankfurt; <sup>2</sup>GSF Darmstadt

## 1 $\phi$ production in central Pb+Pb collisions at 40, 80, and 158 AGeV

In the context of the NA49 energy scan program, the  $\phi$  meson as a carrier of hidden strangeness has been investigated in the  $K^+K^-$  decay channel. Similar to the 158 AGeV data, the position and width of the invariant mass signal at 40 and 80 AGeV are compatible with the book values. The transverse momentum spectra are obtained in the rapidity range of one unit above midrapidity. The slopes obtained by a fit of thermal distributions are  $(244 \pm 10)$  MeV for both 40 and 80 AGeV beam energy, thus considerably lower than at full SPS energy ( $(305 \pm 25)$  MeV).

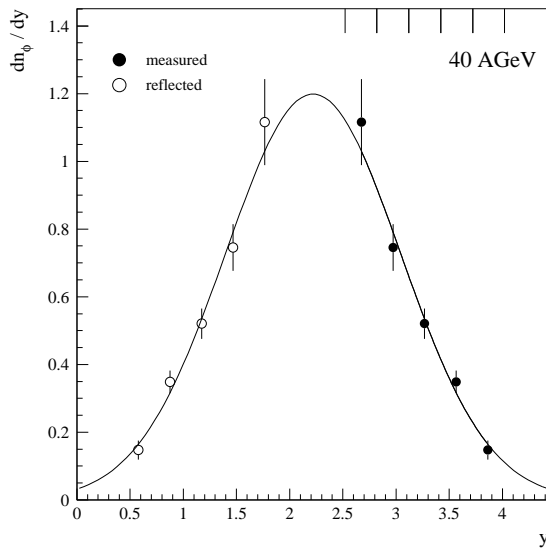


Figure 1: The rapidity distribution of  $\phi$  in central Pb+Pb reactions at 40 AGeV.

Figures 1, 2 show the rapidity distributions for the two energies. They are reasonably well described by a Gaussian. By extrapolation of the measured yield to the full rapidity range, one obtains the total yield which is plotted as function of the center-of-mass energy in the nucleon-nucleon system in Fig. 3. Comparing the energy dependence of  $\phi$  and  $K^-$  production one finds the ratio of  $\langle\phi\rangle$  to  $\langle K^- \rangle$  to be approximately independent of the beam energy. This statement still holds when taking into account AGS and RHIC data.

## 2 $\Omega^-$ and $\bar{\Omega}^+$ production in central Pb+Pb collisions at 158 AGeV

From the  $3 \cdot 10^6$  Pb+Pb events measured in the year 2000 (20% most central part of the total cross section)

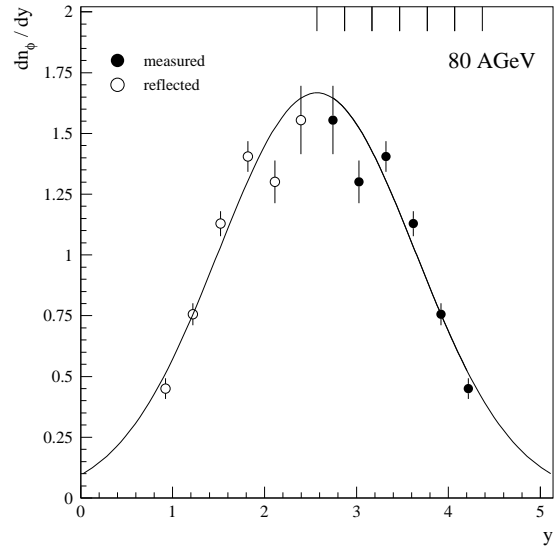


Figure 2: The rapidity distribution of  $\phi$  in central Pb+Pb reactions at 80 AGeV.

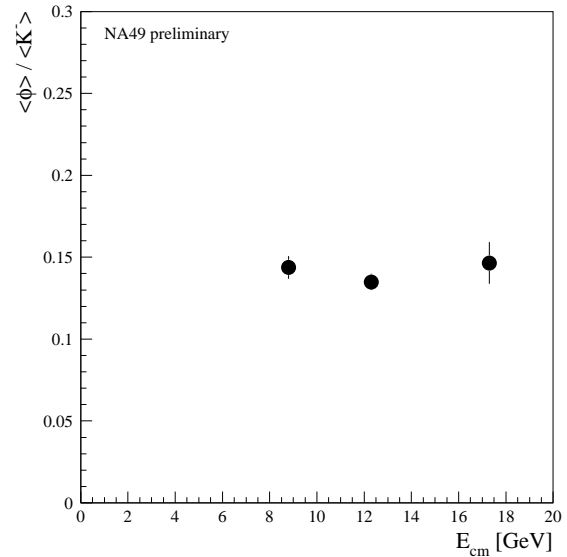


Figure 3: The ratio of the total yields of  $\phi$  and charged Kaons in central Pb+Pb reactions as a function of beam energy.

$\Omega^-$  and  $\bar{\Omega}^+$  were reconstructed via their charged decay branch ( $\Omega^- \rightarrow \Lambda K^-$ , resp.  $\bar{\Omega}^+ \rightarrow \bar{\Lambda} K^+$ ). Figure 4 shows the final invariant mass spectrum for the sum of  $\Omega^-$  and  $\bar{\Omega}^+$  integrated over the accepted phase space region.

The relatively large sample of reconstructed  $\Omega^-$  ( $\bar{\Omega}^+$ )

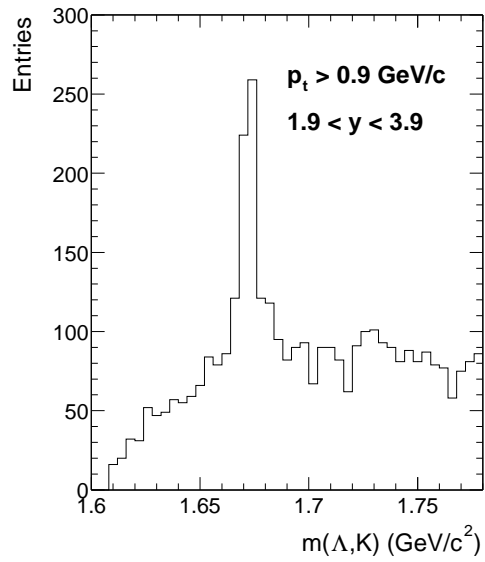


Figure 4: The invariant mass distribution of  $\Lambda K^-$  and  $\bar{\Lambda} K^+$  pairs for central Pb+Pb reactions at 158 AGeV. The signal is integrated over the phase space region  $p_t > 0.9$  GeV/c and  $1.9 < y < 3.9$ .

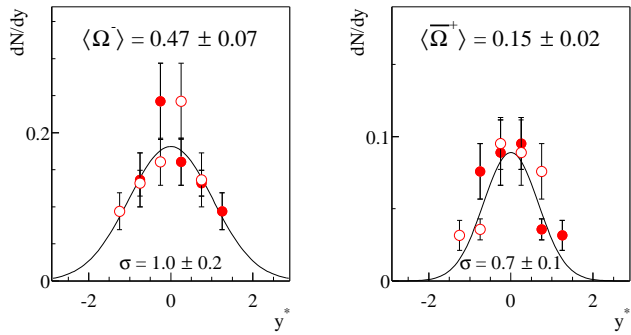


Figure 5: The rapidity spectra of  $\Omega^-$  and  $\bar{\Omega}^+$  in central Pb+Pb reactions at 158 AGeV. The full symbols are the measured data points, while the open ones show their reflection around midrapidity. The total yields were extracted by integrating the Gaussian fits (full lines).

allows for the first time to derive a longitudinal spectrum of both, particle and anti-particle. Figure 5 shows the resulting spectra. The data points include a correction for acceptance and reconstruction efficiency in the high multiplicity environment of a central Pb+Pb event. The corresponding  $m_t$ -spectra are discussed in section 3.

The measured rapidity distribution can be reasonably well described by a Gauss function. The fit to the data points reveals that the width of the distribution appears to be narrower for the  $\bar{\Omega}^+$  ( $\sigma = 0.7 \pm 0.1$ ) than for the  $\Omega^-$  ( $\sigma = 1.0 \pm 0.2$ ). By integrating these Gaussian fits values for the total yields can be extracted. The resulting values are  $\langle \Omega^- \rangle = 0.47 \pm 0.07$  and  $\langle \bar{\Omega}^+ \rangle = 0.15 \pm 0.02$ , corresponding to an  $\bar{\Omega}^+ / \Omega^-$ -ratio significantly below 1. The midrapidity yields are compatible to earlier measure-

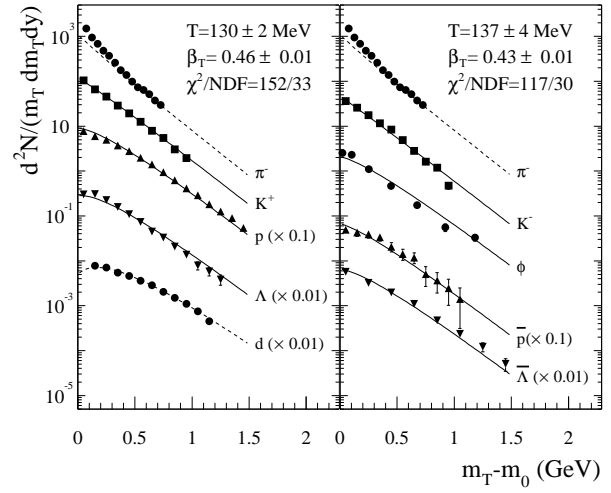


Figure 6: Transverse mass spectra in central Pb+Pb collisions at 40 AGeV. The lines represent the result of a fit with a model that includes transverse expansion.

ments [1], if the different centrality selection is taken into account.

### 3 Transverse mass spectra in central Pb+Pb collisions at 40, 80, and 158 AGeV

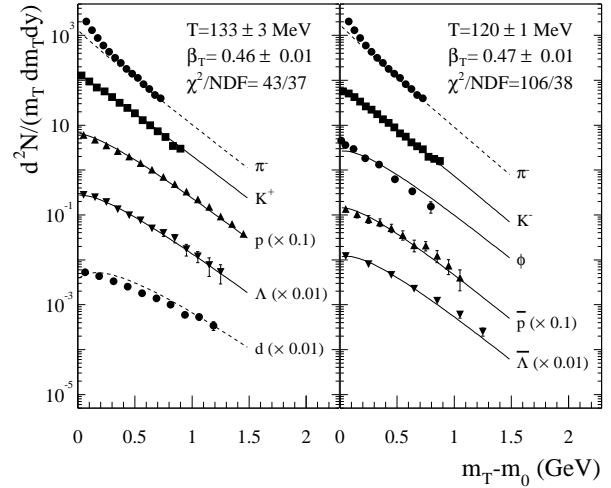


Figure 7: Transverse mass spectra in central Pb+Pb collisions at 80 AGeV.

The figures 6,7,8 summarize the currently available results on transverse mass spectra for a large variety of particles. All spectra are measured at or close to midrapidity, except for the  $\phi$ ,  $\Xi$ , and  $\Omega$ , which are integrated over approximately one unit of rapidity.

In an attempt to provide a universal description of all spectra, the following function, which is based on a hydrodynamical picture and includes transverse expansion [2],

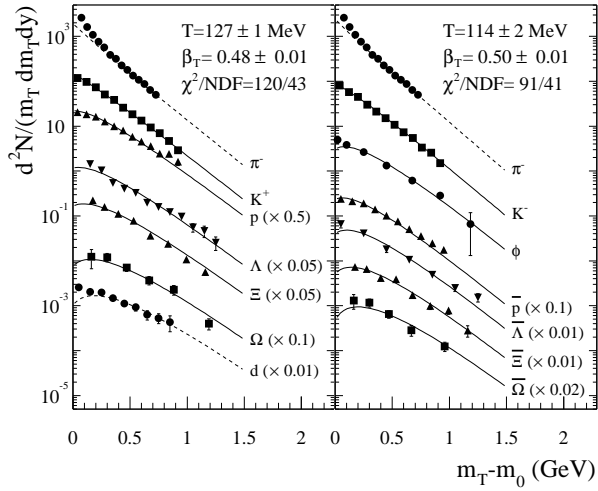


Figure 8: Transverse mass spectra in central Pb+Pb collisions at 158 AGeV.

is fitted to the data [3]:

$$\frac{dN}{m_t dm_t dy} \propto m_t K_1 \left( \frac{m_t \cosh \rho}{T} \right) I_0 \left( \frac{p_t \sinh \rho}{T} \right) \quad (1)$$

By fitting several particle species simultaneously, a thermal freeze-out temperature, as well as a mean transverse flow velocity  $\beta_T$  ( $\rho = \tanh^{-1} \beta_T$ ) can be extracted. The  $\pi^-$  and deuteron spectra were excluded from the fit (dashed lines in Figs. 6,7,8), since the pion spectra are dominated by resonance decays for, especially for lower  $m_t$ , and the deuterons are formed by coalescence. The fit was performed independently for particles (upper row of Figs. 6,7,8) and anti-particles +  $\phi$  (lower row of Figs. 6,7,8). The resulting fit parameter  $T$  and  $\beta_T$  do not exhibit any clear energy dependence, but are all in accordance with a freeze-out temperature of  $T = 115 - 130$  MeV and a transverse expansion velocity of  $\beta_T = 0.4 - 0.5$ . What is remarkable here is the fact that also  $\Omega^-$  ( $\bar{\Omega}^+$ ) data points agree quite reasonable to the fit (see Fig.8). This is in contrast to the usual assumption of an earlier freeze-out of the  $\Omega$ , due to its small cross section with the surrounding hadronic matter [4, 5]. However, if instead of a hydro-dynamical model a simple exponential is fitted to the  $\Omega$  spectra, a  $T$  parameter is extracted that quite low (270 - 290 MeV). in agreement to previous measurements [6].

#### 4 $\Lambda$ and $\bar{\Lambda}$ production in C+C collisions at 158 AGeV

Experimental data on hyperon production with different size nuclei provides information on the system size dependence of strange particle yields and the nuclear stopping power. With this in mind NA49 has analysed Lambda and Antilambda hyperons in central Pb+Pb, Si+Si, C+C and p+p interactions at 158 AGeV. The results of this study are summarized in the figures 9. The left hand side of Fig. 9 shows the rapidity distributions of Lambdas (per

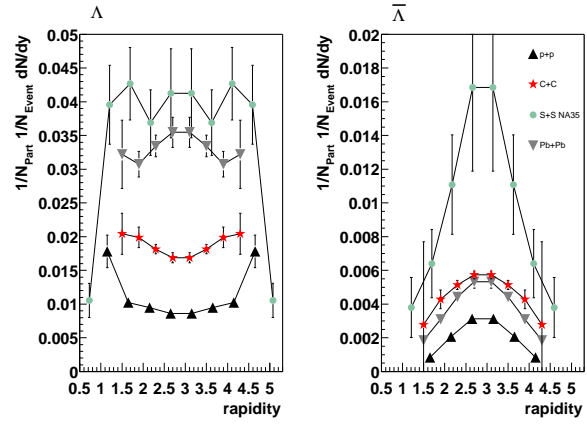


Figure 9: The rapidity distributions of  $\Lambda$  and  $\bar{\Lambda}$  in p+p, central C+C, S+S and Pb+Pb reactions at 158 AGeV normalized to the number of wounded nucleons.

event and per unit of rapidity) normalized to the number of wounded nucleons for the four different systems. Also shown are the published results from S+S collisions [7]. The small systems are characterized by preferred forward and backward Lambda emission, whereas in the heaviest system the rapidity distribution is flat in the region accessible by our our experiment. The change in shape reflects the variation of the nuclear stopping power with system size. The yield per nucleon increases with system size with the largest jump occurring when going from p+p to C+C collisions. No sign of further increase between S+S and Pb+Pb is observed. The rapidity distribution of Antilambda production is shown on the right panel of Fig. 9. No significant change of shape with system size is visible. The yield per participant increases roughly by a factor of two from p+p to central C+C and Pb+Pb collisions. The result from S+S collisions is significantly higher although hampered by large errors. The large difference in yield per nucleon needs to be scrutinized in terms of feed down correction, centre-of-mass energy difference and upcoming results from Si+Si collisions.

#### References

- [1] E. Andersen et al., Phys. Lett. B **449** (1999) 401.
- [2] E. Schnedermann and U.W. Heinz, Phys. Rev. C **50** (1994) 1675 [arXiv:nucl-th/9402018].
- [3] M. van Leeuwen et al. (for the NA49 collaboration), [arXiv:nucl-ex/0208014].
- [4] H. van Hecke, H. Sorge, and N. Xu, Phys. Rev. Lett. **81** (1998) 5764 [arXiv:nucl-th/9804035].
- [5] A. Dumitru, S.A. Bass, M. Bleicher, H. Stöcker, and W. Greiner, Phys. Lett. B **460** (1999) 411 [arXiv:nucl-th/9901046].
- [6] F. Antinori et al. (WA97 collaboration) Eur. Phys. J. C **14** (2000) 633.
- [7] T. Alber et al. (NA35 collaboration) Z. Phys. C **64** (1994) 195.